sustainability

MDPI

Article

Achieving Pareto Optimum for Hybrid Geothermal–Solar (PV)–Gas Heating Systems: Minimising Lifecycle Cost and Greenhouse Gas Emissions

Yu Zhou [1,2,3], Guillermo A. Narsilio [3], Kenichi Soga [4] and Lu Aye [3,*]

[1] Peking University HSBC Business School, University Town, Peking Campus, Lishui Rd., Shenzhen 518055, China; yu.zhou@phbs.pku.edu.cn or zhouyu@gbishenzhen.com
[2] Shenzhen Greater Bay Financial Institute, Baisong Rd., Longhua District, Shenzhen 518000, China
[3] Department of Infrastructure Engineering, Faculty of Engineering and Information Technology, University of Melbourne, Melbourne, VIC 3010, Australia; nasilio@unimelb.edu.au
[4] Department of Civil and Environmental Engineering, University of California-Berkeley, Berkeley, CA 94701, USA; soga@berkeley.edu
* Correspondence: lua@unimelb.edu.au

Abstract: This article investigates heating options for poultry houses (or sheds) in order to meet their specific indoor air temperature requirements, with case studies conducted across Australia under conditions similar to those encountered worldwide. Hybrid geothermal–solar (PV)–gas heating systems with various configurations are proposed to minimise the lifecycle costs and GHG emissions of poultry shed heating, which involves six seven-week cycles per year. The baseload heating demand is satisfied using ground-source heat pumps (GSHPs), with solar photovoltaic panels generating the electricity needed. LPG burners satisfy the remaining heating demand. Integrating these systems with GSHPs aims to minimise the overall installation costs of the heating system. The primary focus is to curtail the costs and GHG emissions of poultry shed heating with these hybrid systems, considering three different electricity offsetting scenarios. It is found that a considerable reduction in the lifecycle cost (up to 55%) and GHG emissions (up to 50%) can be achieved when hybrid systems are used for heating. The Pareto front solutions for the systems are also determined. By comparing the Pareto front solutions for various scenarios, it is found that the shave factor, a measure of the GSHP proportion of the overall system, significantly influences the lifecycle cost, while the size and utilisation of the solar PV panels significantly affect the lifecycle GHG emissions.

Keywords: building performance simulation; geothermal energy; multi-objective optimisation; poultry sheds; solar PV; lifecycle analysis; hybrid renewable energy systems

Citation: Zhou, Y.; Narsilio, G.A.; Soga, K.; Aye, L. Achieving Pareto Optimum for Hybrid Geothermal–Solar (PV)–Gas Heating Systems: Minimising Lifecycle Cost and Greenhouse Gas Emissions. *Sustainability* **2024**, *16*, 6595. https://doi.org/10.3390/su16156595

Academic Editor: Quetzalcoatl Hernández-Escobedo

Received: 2 July 2024
Revised: 24 July 2024
Accepted: 30 July 2024
Published: 1 August 2024

1. Introduction

Ground-source heat pump (GSHP) systems can provide space heating with a lower carbon footprint than best practice gas heaters by utilising thermal energy from the ground [1]. A GSHP system typically incorporates a heat pump, an associated ground heat exchanger (GHE) field, and a distribution system. Recent years have witnessed various applications of GSHP systems worldwide, spanning from residential to commercial buildings [2,3]. The adoption of GSHP technology is relatively high in various countries, including the United States, China, Canada, and Sweden [4], but its utilisation for poultry shed heating is a relatively recent trend [5,6]. While GSHP systems can have high upfront construction costs and GHG emissions, these issues can be mitigated by integrating GSHPs with other energy sources to create a hybrid system [7–10]. Prior research has demonstrated that hybrid geothermal systems can not only be financially beneficial but also assist in balancing thermal loads within the ground [11–17]. Agriculture is one potential area where hybrid geothermal systems can reduce energy consumption and GHG emissions. Worldwide,

agriculture contributes almost USD 5 trillion to the global economy (~6.4% of the gross domestic product GDP), with a significant amount of energy being consumed and emissions being produced [18].

While a wide range of applications for hybrid geothermal systems have been investigated [11–17], they are mainly for residential and commercial buildings with different thermal load patterns to rural industries. This difference in load pattern can have a significant impact on the performance of hybrid geothermal systems. There are no detailed studies currently available regarding the optimisation of hybrid geothermal systems under rural industries' loading conditions. This study aims to address this issue and contribute to the widespread application of hybrid geothermal systems in the agriculture sector.

This research covers the potential use of hybrid systems under a range of climatic conditions encountered worldwide and for typical (best practice) poultry shed envelops. The study is exemplified using case studies from the Australian poultry industry, a sector that contributes significantly to the country's agricultural GDP, accounting for 12% of the national total [19,20]. Nationally, it is estimated that between 600 and 800 million chickens are raised annually in the poultry industry [21]. Given its vast scale, the poultry industry consumes a considerable amount of energy and generates greenhouse gas (GHG) emissions, particularly for the heating and cooling of poultry sheds. It is estimated that approximately AUD 80 million is spent yearly on these operations, accompanied by significant GHG emissions [22]. With the adoption of energy-efficient and renewable heating and cooling systems, the operating costs of farming could be reduced. Given that existing cooling systems for chicken sheds, such as evaporative cooling, are cost-effective and generate relatively low GHG emissions, this study primarily aimed to minimise the costs and GHG emissions associated with heating poultry sheds.

Articulated natural gas and bottled liquefied petroleum gas (LPG) are the predominant heating sources in Australia [23] and various other regions globally. These fossil fuels are not only expensive but also emit substantial GHG emissions upon combustion (approximately 0.186 kg CO_2-e per kW·h) [24]. To address these issues, this study proposes the introduction of high-performance equipment that utilises renewable and sustainable energy sources, either through new construction or by refurbishing and partially replacing existing gas heating systems, to reduce lifecycle costs and GHG emissions significantly. Furthermore, to further lower the operating costs of GSHP systems, solar photovoltaic (PV) systems can be implemented to offset the electricity consumed by the GSHP systems, which will also help to reduce GHG emissions. In previous studies, while solar thermal collectors have been used to enhance the performance of GSHP systems, improving it by up to 10% [9,16,25–28], the benefits of solar PV systems are even more significant, offering up to 100% savings in operating costs [29]. Therefore, in this study, only solar PV systems were employed and analysed. By combining these three energy sources, this study aimed to achieve significant reductions in both costs and GHG emissions [30,31]. The proposed hybrid geothermal–solar (PV)–gas heating system holds the potential to considerably lower operating and lifecycle heating costs, along with associated GHG emissions [29]. This study further investigated the influence of the size of the components of these systems (GSHPs, solar PV systems, and gas burners) to determine the optimum system configurations.

Despite the widespread adoption of ground-source heat pump (GSHP) systems for space heating in various applications worldwide, there is a notable research gap regarding their utilisation and optimisation in rural industries, particularly in the agriculture sector. While hybrid geothermal systems have shown promise in reducing energy consumption and greenhouse gas (GHG) emissions in residential and commercial buildings, their potential under rural industries' loading conditions remains unexplored. This study aimed to address this gap by investigating the use of hybrid geothermal systems in the poultry industry, specifically focusing on poultry shed heating. By examining the potential of integrating GSHPs with solar photovoltaic (PV) systems and gas heaters, this research sought to determine the optimum system configurations that can significantly reduce both lifecycle heating costs and associated GHG emissions.

This study identified the Pareto front solutions for minimising the lifecycle cost and lifecycle GHG emissions of hybrid geothermal–solar (PV)–gas heating systems. It discusses the optimisation of the systems for typical chicken sheds in Central Coast, New South Wales (NSW), Sunshine Coast, Queensland (QLD), and Mornington Peninsula, Victoria (VIC), where more than 74% of Australian chicken meat is produced and a range of climatic conditions are encountered, thus covering situations similar to those found around the world where chicken meat is produced. Utilising Transient System Simulation Tool (TRNSYS) 18, a comprehensive building energy simulation model was developed to replicate typical sheds, and it was verified by comparing its predictions with current energy consumption data. Because agriculture investment in infrastructure is usually a long-term investment (typically with a 50-year horizon), an in-depth 40-year lifecycle analysis was conducted based on this building performance simulation. This analysis encompassed optimisation considering the installed capacities of the various components within the hybrid geothermal–solar (PV)–gas heating systems. Given that the expected lifespan of ground heat exchangers and sheds typically exceeds 40 years, this study adopted a 40-year lifecycle as the reference period for analysis.

2. Methods and Data

The methods employed in this study and the key data used for each representative shed, climate, and operation are summarised in this section and outlined in Figure 1.

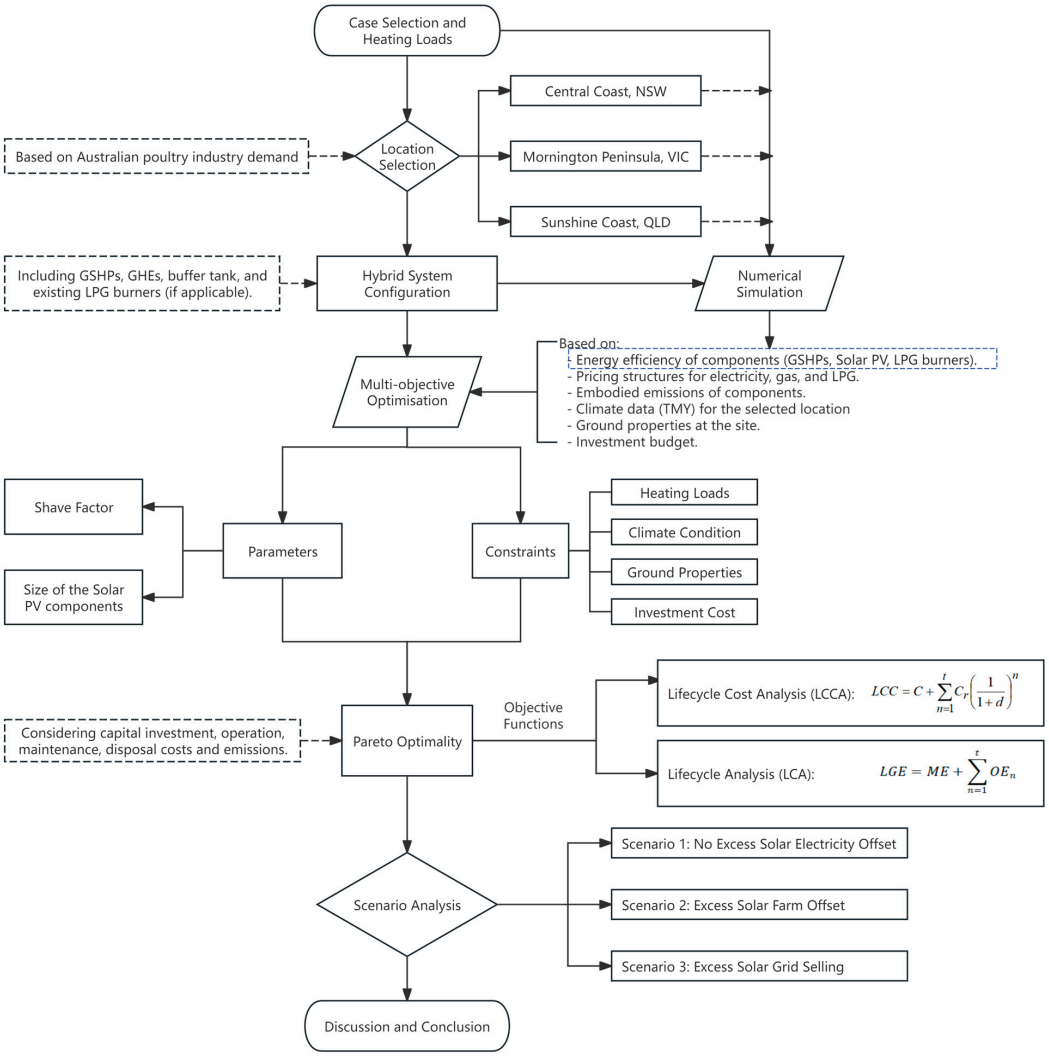

Figure 1. Schematic flowchart of methods for multi-objective optimisation.

This study began with a demand analysis to determine energy requirements and consider the location of the industry (Section 2.1). Then, a hybrid system consisting of solar photovoltaic (PV) modules, batteries, buffer tanks, and existing liquefied petroleum gas (LPG) burners was configured (Sections 2.2 and 2.3). The system was optimised based on multiple objective functions (Section 2.4), i.e., a lifecycle cost analysis (LCCA) considering investment, operation, maintenance, and disposal costs, as well as a lifecycle analysis (LCA) with parameters and constraints (Section 2.5). Finally, three different scenarios for the utilisation of solar PV are discussed (Section 2.6).

2.1. Poultry Shed: Location, Construction, Operation, and Climate

Three different locations across Australia were selected to study the optimal configurations of the hybrid system for analogous poultry sheds under different climatic conditions. The three locations represent New South Wales (NSW), Victoria (VIC), and Queensland (QLD) (Figure 1). These three states account for 74.4% of Australian national broiler production [32] and cover the humid subtropical and temperate oceanic climate conditions, which can be suitable for raising poultry [32–35], and they are used to exemplify similar conditions encountered around the world.

The specific locations and the latest average yearly summer and winter temperatures are presented in Table 1. The undisturbed ground temperature was estimated based on the annual mean outdoor temperature. All the other factors for each location were held constant in this study.

Table 1. Simulation locations and key climate data for Australia [36,37].

Location	Coordinates	Annual Mean Maximum Temperature (°C)	Annual Mean Minimum Temperature (°C)	Undisturbed Ground Temperature (°C)
Central Coast, NSW	33°23′49″ S 150°24′09″ E	21.9	11.6	16.1
Mornington Peninsula, VIC	38°17′7″ S 145°5′36″ E	18.9	10.1	14.4
Sunshine Coast, QLD	26°51′36″ S 152°57′36″ E	25.3	17.0	19.9

A poultry shed in Peats Ridge in Central Coast, NSW (Australia), was first investigated as an example in a temperate climate region. Data from existing sheds operating at this location were used as a base case. The key specifications of the shed are outlined in Table 2. To assess its energy performance, a TRNSYS building energy simulation model was established [38,39]. This model simulated the annual heating and cooling demands of the shed. The performance data of the components, including the GSHP and solar PV system, were derived from equipment available on the Australian market in the early 2020s.

Table 2. Poultry shed parameters [38,39].

Dimensions	Width: 18.3 m; Length: 138.7 m; Height: 2.7 to 4.3 m
Wall/Roof Material	No windows; insulation with thin layers of metal claddingInsulation thickness: 0.075 m; thermal conductivity: 0.039 $Wm^{-1}K^{-1}$; density: 16 kgm^{-3}; specific heat: 340 $Jkg^{-1}K^{-1}$
Orientation	Long axis (length) from north to south
Location	Peats Ridge, NSW, Australia (33°23′49″ S, 150°24′09″ E)
Climate Data	Typical Meteorological Year (TMY) data [36]

It has been reported that the operating schedule of chicken sheds is an important factor and can affect heating energy consumption [22,29,38]. This study assumed a January 1st start for the first batch, with six batches annually, each lasting 7 weeks with a 2-week break. Each batch began with 50,000 chickens, harvested in three stages: 15,000 at week 5, 10,000 at week 6, and 25,000 at week 7. Chicken mortality was not factored in due to a lack

of reliable data. Weight gain and heat generation data for the chickens, aligning with the Peats Ridge shed owner and operator recommendations (and assumed to be the same for the other locations for ease of comparison), are provided in Table 3.

Table 3. Chicken growth and metabolic heat generation [29].

Day of Growth Cycle	Mass per Chicken (kg)	Heat Generation per Chicken (W)	Number of Chickens (-)	Indoor Setpoint Temperature (°C)
1	0.054	0.82	50,000	31.0
7	0.180	2.02	50,000	28.6
14	0.438	3.93	50,000	26.1
21	0.829	6.34	50,000	23.7
28	1.337	9.08	50,000	21.2
35	1.897	11.80	50,000	19.0
42	2.444	14.27	35,000	19.0
49	2.873	16.11	25,000	19.0

2.2. Hybrid System: Configuration and Shave Factor

Figure 2 depicts a hybrid geothermal–solar (PV)–gas heating system configuration that incorporates multiple identical GSHPs arranged in parallel to a main header pipe. Each GSHP is interconnected with a series of GHEs [39], and, downstream, they are linked to a buffer tank to mitigate the frequent on–off cycling of the heat pumps. Existing LPG burners installed in the shed in NSW can provide supplemental heating whenever necessary. Currently, this shed relies solely on LPG burners for heating, and the simulation model was verified with LPG purchase receipts for two years provided by the farm owner [22,29,38]. By adjusting the ventilation rate, which represents the air exchange rate with the outdoor environment, the actual LPG consumption could be closely aligned with the calculated annual heating costs, using a calibrated ventilation rate of 1.04×10^{-4} $m^3 \cdot s^{-1} \cdot kg^{-1}$ [40].

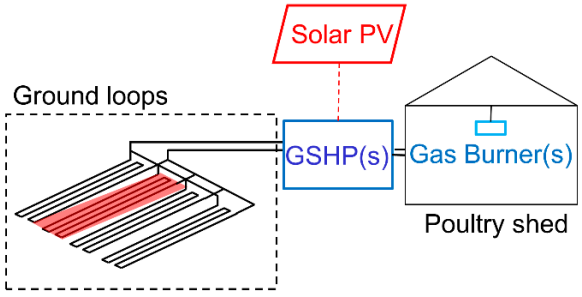

Figure 2. Schematic representation of a hybrid geothermal–solar (PV)–gas system.

The hybrid system employs multiple 20 kW single-speed GSHPs, each with a fixed ground heat exchanger field comprising four 75 m long trenches at a 1.5 m depth. Each trench holds four straight pipes, spaced 300 mm apart, as depicted in Figure 3. The system operates based on hourly heating demands, prioritising heat pumps with lower accumulated hours. For demands exceeding GSHP capacity, gas burners provide the balance.

The "shave factor" S quantifies the GSHP capacity in a hybrid system, representing the ratio of the GSHP installed capacity to the estimated peak heating demand (Equation (1)) [11,15]. In this study, a 0% shave factor signifies a full gas system, while 100% indicates a full GSHP system [22,29,38]:

$$S = \frac{\text{Installed capacity of GSHP}}{\text{Peak heating load}} \times 100\% \quad (1)$$

For instance, a 60% shave factor in a geothermal–gas hybrid system with a 208 kW peak load demand implies a GSHP installed capacity of 125 kW, with the remaining 83 kW provided by gas burners.

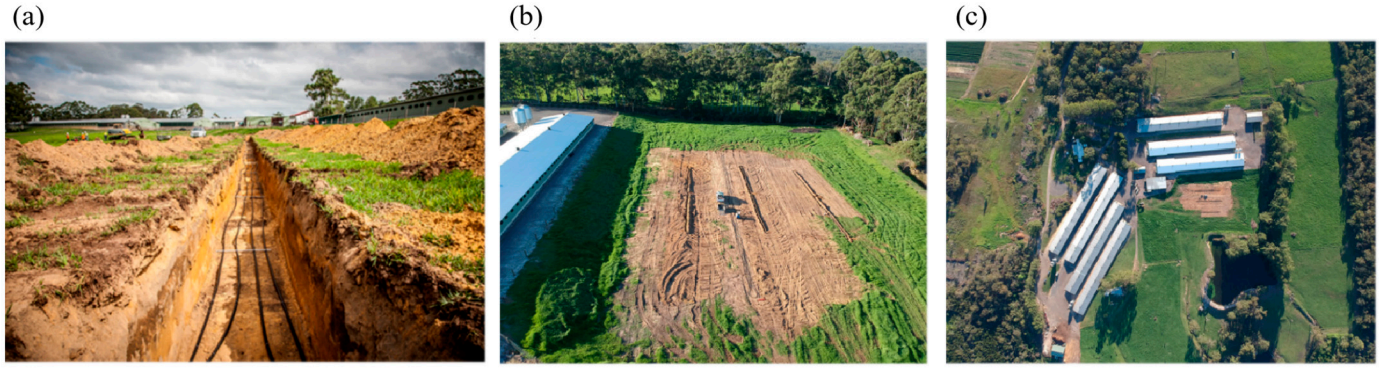

Figure 3. Images of a full-scale hybrid system being installed in Central Coast, NSW: (**a**) A GHE pipe and 0.5 m width trench configuration. (**b**) A view of the approximately 30 m × 60 m GHE field. (**c**) A top view of the whole farm.

2.3. Hybrid System Components: Efficiency, Pricing, and Embodied Emissions

To optimise the costs and emissions of the hybrid system(s), comprehensive data on the energy efficiency, pricing structures, and GHG emissions of each core component within the proposed hybrid system are imperative. Table 4 outlines the energy pricing framework adopted for this optimisation process.

Table 4. Energy prices of gas and electricity for investigated systems.

	NSW	NSW SME	QLD SME	VIC SME
Electricity Price, c/(kW·h)	10	31.2	29.8	24.3
Gas Price, AUD/GJ	19.5 (LPG)	26	35	18

The energy prices specific to NSW are derived from the current energy contracts held by the Peats Ridge NSW farm owner. It is noteworthy that gas and electricity prices can vary among farms, primarily due to their individual contracts with suppliers. The electricity usage cost for this particular farm is considered competitive, attributed to the relatively high fixed supply charges incorporated in the contract. The fixed supply charge for electricity and gas is not considered in the lifecycle analysis because the fixed charge should be paid regardless of whether a hybrid system is installed, and it is similar to land taxes or council rates. The average electricity prices in QLD and VIC are obtained from reports by Jacobs and Alviss Consulting as average prices for Small and Medium Enterprises (SMEs) [41,42].

The annual average efficiency of LPG burners is assumed based on the equipment available on the market in Australia in the early 2020s. The coefficient of performance (COP) of heat pumps can vary significantly under different operating conditions. Therefore, a simulation model in TRNSYS is developed to determine the hourly variation in the GSHP heating COP.

Solar PV modules convert radiation from the sun into electricity. This study proposes the installation of solar PV modules to generate electricity specifically for the shed heating system. The hourly electricity generated per square metre of solar PV panels is computed using weather data from a Typical Meteorological Year (TMY) and following the steps detailed in Appendix A. Three different scenarios are considered regarding the usage of the electricity generated from solar PV panels, namely, (a) a no electricity storage scenario, (b) a farm offset scenario, and (c) a grid selling scenario, and these are detailed in Section 2.6. Various-sized PV arrays were investigated to determine the optimum-sized PV panels under these three scenarios. These scenarios are discussed in Section 2.5. The embodied GHG emission for 1 m^2 of solar PV panels is estimated to be 42 kg/m^2 [43–45].

The GSHPs, along with their associated circulation pumps, which drive fluid through the GHEs, require electricity for their operation. In NSW, the GHG emission associated

with electricity consumption is estimated to be 0.82 kg CO_2-e per kW·h [24]. In this study, a 1% annual reduction in the electricity generation GHG emission factor is assumed, which is grounded in the Australian government's commitment to reducing GHG emissions by 26% to 28% below 2005 levels by 2030, equating to an approximate 1% reduction annually [46]. The GHG emission factor for LPG usage is assumed to remain constant in this study, and it is 0.186 kg CO_2-e per kW·h of energy consumed in NSW [24].

Based on the above information, Table 5 summarises the initial embodied GHG emission of different components, with GSHP and gas burner data calculated from a lifecycle analysis of a standard 10 kW heating system in Australia [47].

Table 5. Initial GHG emissions and lifetime of different components [29].

	GSHP Aboveground Components	GSHP Underground Components	Solar PV	LPG Burner
Initial GHG Emission, kg CO_2-e per kW	67	93.8	42 kg/m^2	10.2
Initial Cost, AUD per kW	750	750	1245	100
Lifecycle, years	20	40	20	10

2.4. Lifecycle Analysis

As outlined in the previous section, adopting a hybrid geothermal–solar (PV)–gas heating system can achieve substantial reductions in operating costs, particularly with the offset of electricity from solar PV modules (up to a 100% cost reduction). However, high operating cost savings are typically related to high capital system investment costs.

In order to balance the initial investment with future financial returns (operating cost savings), financial metrics and methods, such as a lifecycle cost analysis (LCCA), can be employed to make objective investment decisions [10]. An LCCA evaluates the financial feasibility of a project over its lifetime based on net present values, considering the capital investment, operation, maintenance, and disposal costs [48]. Equation (2) serves as the first objective function in this study and calculates the lifecycle cost of the heating system [49]:

$$LCC = C + \sum_{n=1}^{t} C_r \left(\frac{1}{1+d} \right)^n. \quad (2)$$

where LCC is the lifecycle cost; C is the initial capital investment cost; C_r is the recurring cost, including operation, maintenance, and disposal costs, in the n^{th} time period; d is the real discount rate; and t is the lifetime of the project in years.

The initial capital costs and estimated lifespans of the various components used in the analysis, including the LPG heaters, GSHPs, GHEs, and solar PV modules, are outlined in Table 5. These costs are based on current market averages, with LPG heaters, GSHPs, and GHEs being priced per unit heating capacity and solar PV modules being priced per installed peak electricity generation capacity. The total solar PV panel capacity is determined by the system's annual electricity consumption. The sizing of these components is further detailed in Section 2.5. For this analysis, the energy prices and efficiency ratings of the heating system components are assumed to be similar to those in Table 4. The price escalation rate of LPG is set to 6.14%, matching that of natural gas, while electricity's price escalation rate is fixed at 6.20% [47]. Given the project's low-risk nature, the discount rate is set to 5.08%, slightly above the Reserve Bank of Australia's cash rates [50].

In addition, regarding the environmental aspects, the lifecycle GHGs are investigated as the second objective function by following a similar approach:

$$LGE = ME + \sum_{n=1}^{t} OE_n \quad (3)$$

where LGE is the lifecycle GHG emission, ME is the manufacturing GHG emission, OE_n is the operating GHG emission in year n, and t is the project lifetime in years. The initial

GHG emissions and lifetime of the different components are discussed in Section 2.3 and are presented in Table 5.

2.5. Multi-Objective Optimisation PARAMETERS

The overall goal of utilising the geothermal system is to minimise lifecycle costs together with GHG emissions. To achieve this goal, different optimisation parameters and constraints, as well as objective functions, are presented below.

2.5.1. Optimisation Parameters

Two different types of parameters for optimisation are considered here:

1. The size of the GSHP components

As this system is a hybrid system, factors for energy resources are the key parameters for the optimisation:

$$\alpha_{Geo} + \alpha_{LPG} = 100\% \quad (4)$$

where α_{Geo} is the fraction of geothermal energy, and α_{LPG} is the fraction of energy provided by the LPG.

2. The size of the solar PV components

The solar PV panels are installed to provide electricity for the GSHP systems. Different scenarios, including offsetting the electricity using other types of equipment on the farm and selling it to the grid, are also considered in this study.

2.5.2. Constraints of the Optimisation

1. Heating loads

The loading pattern of the poultry shed is the primary constraint, and it is subject to the temperature requirement of the building.

2. Climate condition

The climate condition affects the performance of the solar PV components and the ground temperature, which influences the performance of the GHE. Here, the climate data comprise TMY (Typical Meteorological Year) data for one year. This dataset is generated from 20 years of recorded climate data and can be used as a representative weather dataset. Although the climate condition is not technically a parameter for optimisation, several climate data are used to check the validity of the optimisation representing different cases/locations so as to generalise or highlight the applicability of this technology under different climatic conditions (e.g., would a geothermal system be a better option in a cooler climate?).

3. Ground Properties

The soil properties also limit the performance of GHEs. The land and space availability impact the trench length and the distribution of the pipes.

4. Investment Cost

As the funding is limited, the initial capital costs should be considered budgeted. Meanwhile, the ongoing costs of the hybrid system should at least be less than the previous ones.

2.5.3. Objective Functions for Optimisation

The last stage of this work focuses on the optimisation of the hybrid horizontal geothermal system based on economic and environmental factors. As discussed in Section 2.4, to achieve this goal, first, a lifecycle cost analysis and a lifecycle GHG emission analysis of the hybrid geothermal system are conducted. Accordingly, two different objective functions are employed for the optimisation. The first one focuses on the financial part, i.e., minimising the lifecycle cost, while the second one focuses on the environmental part to minimise the

lifecycle greenhouse gas emissions. The result of this optimisation will help to answer the question "How can a hybrid horizontal geothermal system be optimised for the rural industry based on economic and environmental factors?", as well as provide a better understanding of the geothermal system. The first objective function regarding Lifecycle Cost in Net Present Value is Equation (2) as discussed in Section 2.4 and the second objective function regarding Lifecycle GHG Emissions is as below [49]:

$$LGE = ME + \sum_{n=1}^{t} OE_n \quad (5)$$

where LGE is the lifecycle GHG emissions, ME is the manufacture GHG emissions, OE_n is the operational GHG emissions in year n, and t is the analysis period.

2.6. Different Scenarios for Multi-Objective Optimisation

Using the data and method discussed previously, three different scenarios are considered for determining the Pareto front solutions of the hybrid geothermal–solar (PV)–gas system. The Pareto front solutions are identified based on the two objective functions discussed earlier (i.e., the lifecycle cost and lifecycle GHG emissions).

2.6.1. Scenario 1—No Excess Solar Electricity Offset

In this case, there is no other equipment or system on the farm that consumes or stores the electricity generated by the solar PV panels, apart from the GSHP systems. Therefore, solar electricity cannot be sold to the grid for profit. This means that the extra electricity generated by the solar PV panels that is not consumed by the GSHP systems will be wasted.

2.6.2. Scenario 2—Excess Solar Farm Offset

As solar electricity storage is typically expensive, preliminary results show that additional electrical storage may not be an appealing option. Alternatively, poultry farms in Australia are typically large, have more than one poultry shed (typically five to eight), and include at least one farmhouse. Therefore, it is assumed that the extra electricity generated by the solar panels can be consumed by other equipment or systems on the farm. It is assumed that the farm has a minimum constant electricity consumption of 10 kWh, which means that this is the limit (in our scenarios) of consumption of the excess solar electricity. This number is estimated based on the electricity bill of the reference farm in Peats Ridge. The minimum monthly average hourly demand is 20 kWh (in July). Considering that solar electricity generation only happens during the day, it is assumed that at least 50% of the average demand is always required. However, in this scenario, the electricity still cannot be sold back to the grid, resulting in a waste of electricity generated if it exceeds the demand of the farm.

2.6.3. Scenario 3—Excess Solar Grid Selling

In this scenario, it is assumed that a contract between the farmer and the electricity supplier is established, allowing the farmer to sell electricity to the grid at market-related or minimum governmental-regulated feed-in prices, which, at the time of writing, are 10 c/kWh, 12 c/kWh, and 10 c/kWh in NSW, VIC, and QLD [41,42], respectively. In this case, the electricity generated by the solar PV panels is first consumed by the GSHP systems, and excess electricity is sold to the grid. The profit from selling electricity then pays for the operation and maintenance costs of the hybrid system.

3. Results and Discussion

The results and discussion are summarised in this section. The results for a single case/location are presented, and then the multiple realisations of the thermal loads and climatic conditions investigated are summarised.

3.1. Heating Cycles of Poultry Sheds under Different Climatic Conditions

First, the heating demands that must be satisfied by the proposed system are examined. Figure 4 presents the heating demand results for the shed in Central Coast, NSW, derived from the TRNSYS model (Section 2.1). The model and the results are verified against the measured energy consumption at the site. The annual heating energy demand for the shed stands at 58,477 kWh, with a peak demand of 208 kW. Notably, during each heating cycle, the heating demand peaks at the beginning, coinciding with the chickens generating the least metabolic heat and the indoor temperature requirement being at its highest (Table 2). As the cycle progresses, the heating demand gradually decreases, attributed to the rise in metabolic heat generated by the chickens and the corresponding reduction in the indoor temperature requirement as the batch ages (Table 2).

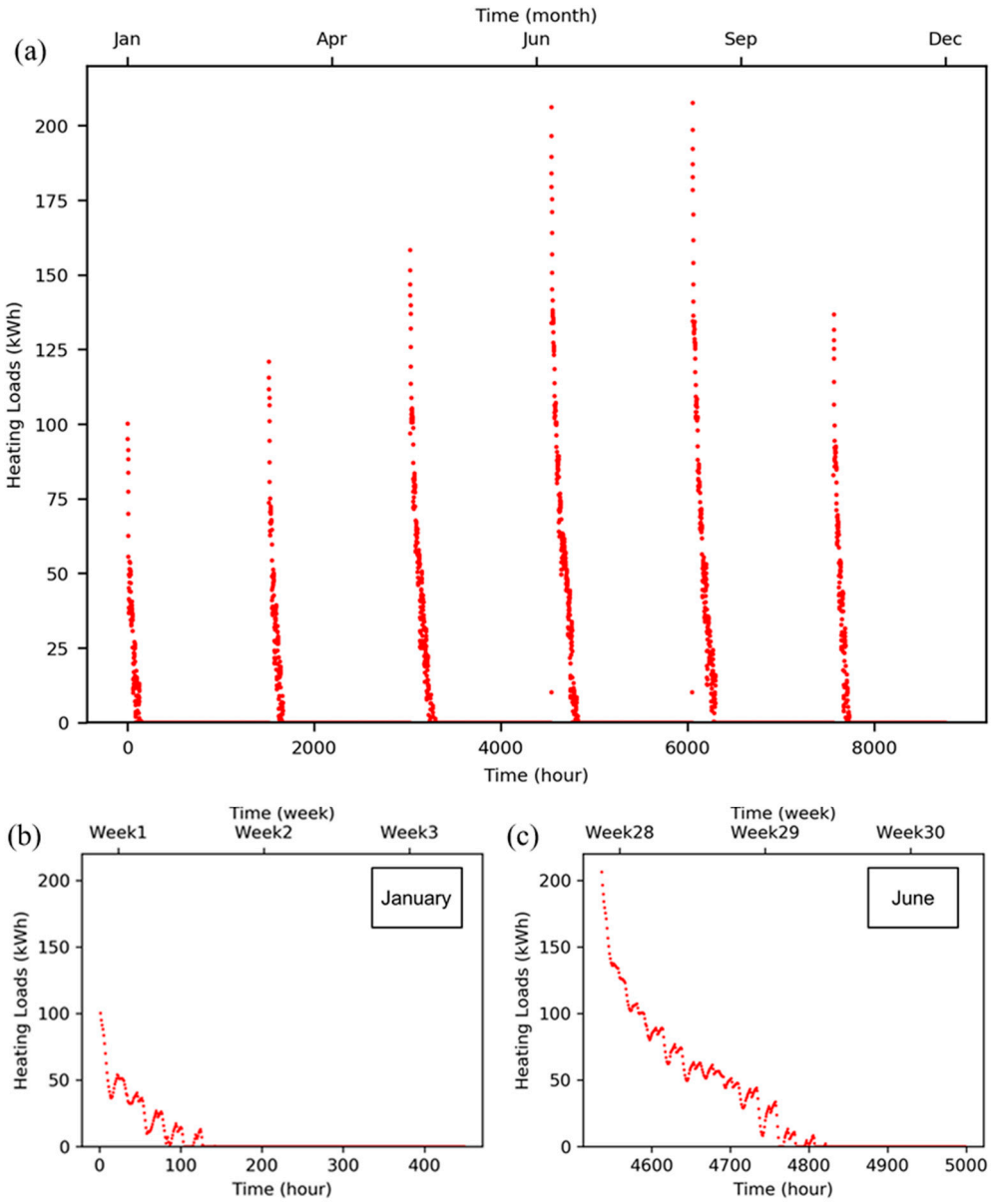

Figure 4. Hourly heating demand of the poultry shed in Central Coast, NSW: (**a**) annual heating demand, (**b**) heating demand for the first cycle, and (**c**) heating demand for the fourth cycle.

The heating load cycles in Sunshine Coast, QLD, and Mornington Peninsula, VIC, exhibit similar patterns, with peak loads of 164 kW and 228 kW and heating demands of

34,149 kWh and 73,456 kWh, respectively. These figures reflect the warmer and cooler climatic environments of QLD and VIC.

Taking the base case shed in NSW, it is noted that the heating demand for the shed remains below 80 kW for a significant portion of the year (as depicted in Figure 4). This underscores the potential benefits of utilising a hybrid heating system. For example, by implementing a system with an installed GSHP capacity comprising approximately 40% (~80 kW) of the peak heating power demand (208 kW), it is estimated that over 90% of the annual heating energy requirements can be met solely by the GSHP. This not only highlights the efficiency of a hybrid heating approach but also demonstrates its cost-effectiveness and reliance on renewable energy resources while requiring significantly less initial capital investment for trenching associated with the GHEs. The next section discusses the efficiency of the components of hybrid systems that could achieve such potential operating cost savings, as well as objective ways to determine the best shave factors.

3.2. Hourly Coefficient of Performance of the GSHPs

As the heating loads vary from hour to hour, the COP of the GSHPs will also vary. The simulation model in TRNSYS is further developed to evaluate the hourly performance of the GSHPs under different shave factors and loading conditions. As detailed in Section 2.2, the system is composed of several identical GSHPs. The system operates based on hourly heating demands, prioritising heat pumps with lower accumulated hours.

For the NSW case study needing a 208 kW total capacity, a thermal loading condition equivalent to a shave factor of approx. 50%—resulting in a GSHP capacity of over 104 kW [38]—necessitates the installation of six 20 kW heat pumps. Each heat pump has a dedicated GHE field in 4 trenches, totalling 24 trenches. When the heating demand exceeds 104 kW, all GSHPs operate simultaneously, and gas burners supply the remaining required energy. The TRNSYS model is executed to simulate the system's performance under these specified conditions. Since the loads are distributed relatively evenly among the six heat pumps, the differences in their performance are not major. Yet, when evaluating the performance of the whole GSHP system, the six heat pumps must be considered as a whole. Therefore, the hourly *system* COP of the heat pumps is calculated based on Equation (6). The hourly *system* COP represents the performance of the whole GSHP system and can be used to calculate the electricity consumed by all the heat pumps hour by hour:

$$COP_{Geo_{hr}} = \frac{\sum_{i=1}^{n} HPQ_i}{\sum_{i=1}^{n} \frac{HPQ_i}{COP_{GSHP_{hr\,i}}}} \quad (6)$$

where n is the number of heat pumps (e.g., n = 6 for the shed case study in Central Coast, NSW, with SF = 50%), HPQ_i is the hourly heating loads covered by each *one* (i^{th}) heat pump in kWh, and $COP_{GSHP_{hr\,i}}$ is the hourly COP for that *one* (i^{th}) heat pump. The hourly electricity consumed $E_{Geo\,hr}$ by all the heat pumps is then calculated based on the hourly system COP as follows:

$$E_{Geo_{hr}} = \frac{\sum_{i=1}^{n} HPQ_i}{COP_{Geo_{hr}}} \quad (7)$$

A factor of 10% is added to consider the electricity consumed by the other equipment, such as the circulating pumps [25,51,52].

As an example of the results, Figure 5 shows the $COP_{GSHP_{hr}}$ for a shave factor of 50% in the case in Central Coast, NSW. Corresponding to the loading pattern shown in Figure 3, there are six operational cycles in a year. The first cycle in the year has the shortest hours of operation (Figure 5b), and the fourth cycle in the year has the longest hours of operation (Figure 5c).

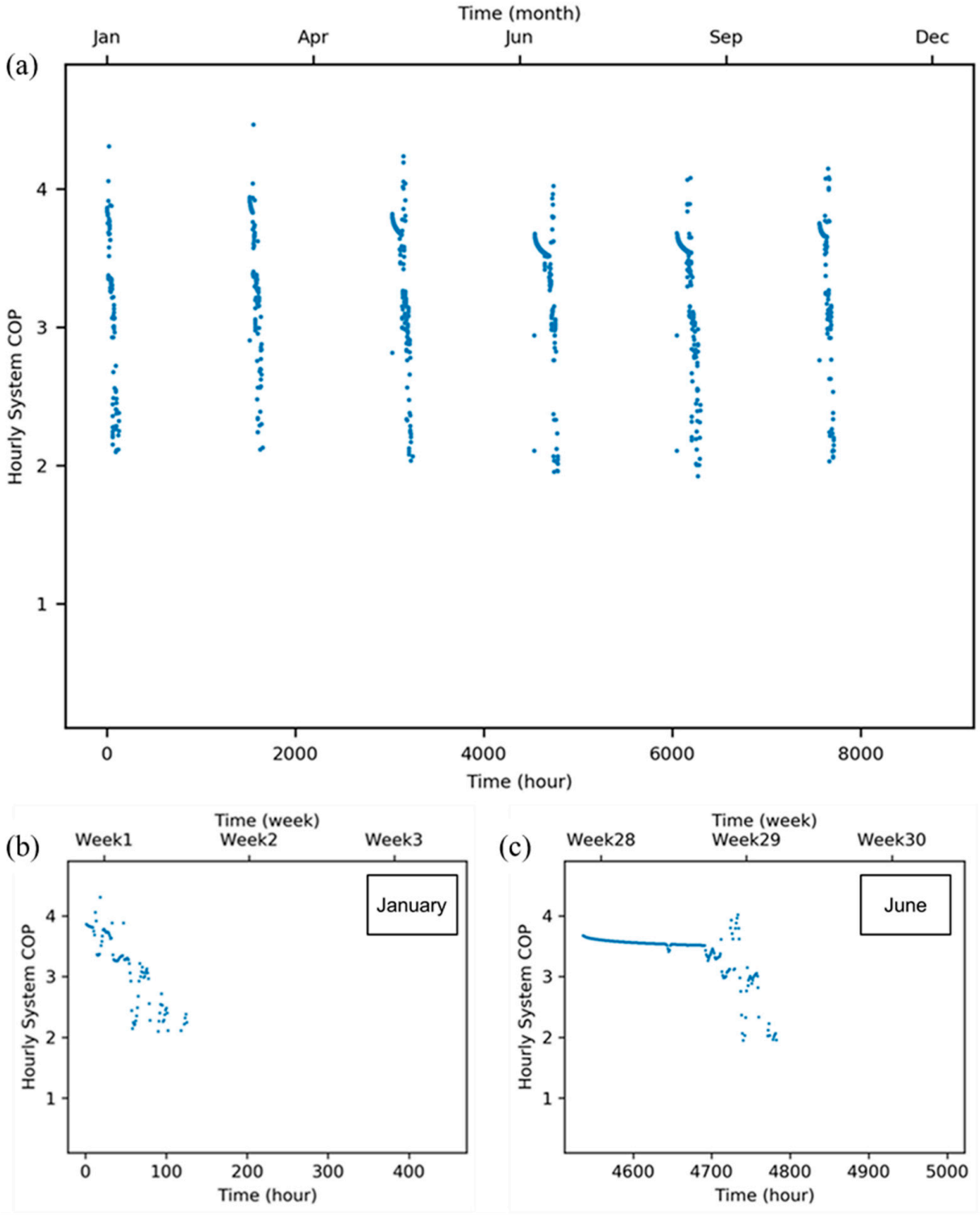

Figure 5. Hourly system COP for 50% shave factor in Central Coast, NSW: (**a**) hourly system COP for the whole year, (**b**) hourly system COP for the first cycle in a year, and (**c**) hourly system COP for the fourth cycle in a year.

The total hourly (t^{th} hour in the year) heating demand for the GSHP system component, TQ_t, is then used together with the hourly system COP, $COP_{Geo_{hr}}$, to estimate the average *annual* COP of the GSHP (geothermal) component COP of the whole hybrid system:

$$COP_{Geo_{annual}} = \frac{\sum_{t=1}^{8760} TQ_t}{\sum_{t=1}^{8760} \frac{TQ_t}{COP_{Geo_{hr\,t}}}} \quad (8)$$

Simulations are conducted for different shave factors (i.e., 25%, 50%, 75%, and 100%). The hourly system COP under the full range of shave factors (from 1% to 100%), which is not explicitly simulated, is estimated via second-order polynomial functions generated from these four data points (the R values for most of the cases are larger than 0.99). Subsequently, the annual system $COP_{Geo_{annual}}$ is calculated based on these hourly system COPs ($COP_{Geo_{hr}}$), as shown in Figure 6, where the results show that, with an increasing shave factor, there is a decrease in the overall COP. The trend observed is counter-intuitive; one would expect an increase in the overall COP with an increasing percentage of use of a more efficient HVAC system (the GSHPs). The decrease rate also becomes slower as the shave factor becomes higher. Based on the heating loads presented in Section 3.1, it is determined that this decreasing COP is caused by the increasing overall running time, with chances of the partial loading of the heat pumps as the shave factor increases. The partial loading condition significantly reduces the COP of the individual heat pumps [46,53,54].

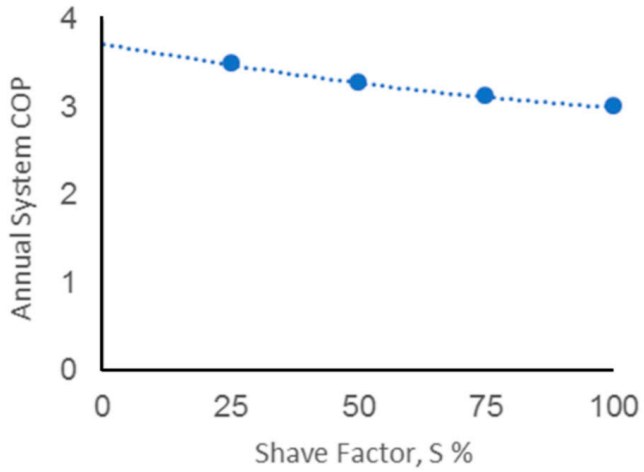

Figure 6. Annual system COP ($COP_{Geo_{annual}}$) under the full range of shave factors for the NSW shed case study.

3.3. Lifecycle Analysis: Costs and GHG Emissions

Using the data and method discussed previously, the results of the three different scenarios introduced in Section 2.6 are presented in detail for the NSW's hybrid geothermal–solar (PV)–gas system, and they are also discussed. Summaries of the Pareto front solutions for the other climatic conditions are included in the next section.

3.3.1. Scenario 1—No Excess Solar Electricity Offset

In Scenario 1, there is no other equipment or system on the farm that can consume (or store) the electricity generated by the solar PV panels, apart from the GSHP systems.

Regarding the lifecycle costs obtained from Equation (2) for the case study in Central Coast, NSW (Figure 7a), the results show that the shave factor has a greater impact than the solar PV size on costs. The optimum shave factor is found to be approximately 20% to 25%, and the optimum solar PV size under this condition is approximately 0 to 50 m^2. For the lifecycle GHG emissions (Figure 7b), the solar PV size becomes more important when the shave factor is greater than 20%. The optimum shave factor here is approximately 30% to 35%; however, the optimum solar PV size increases to 220–245 m^2.

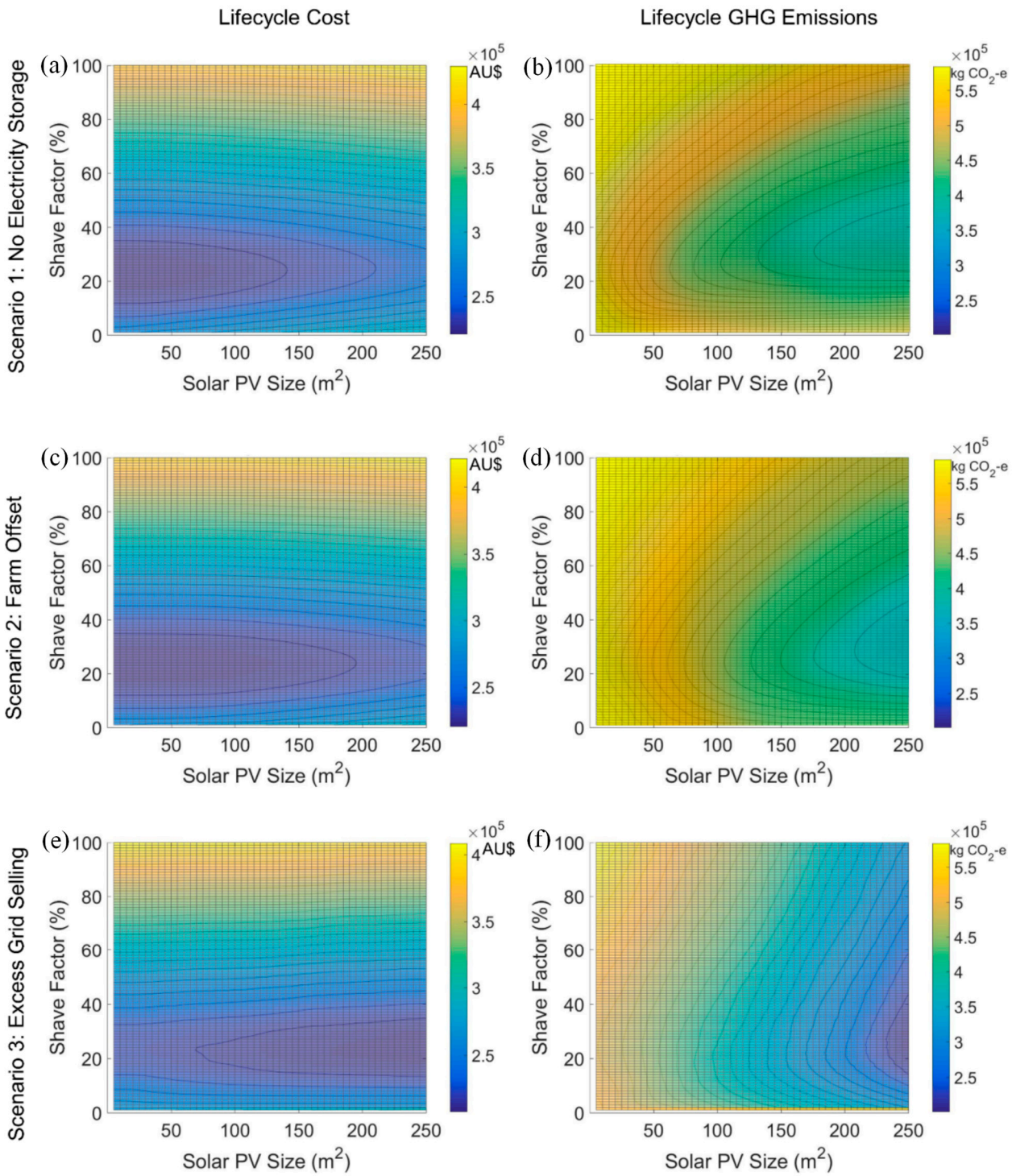

Figure 7. Lifecycle costs and GHG emissions of three scenarios in Central Coast, NSW:(**a**) Lifecycle cost for Scenario 1; (**b**) Lifecycle GHG emission for Scenario 1; (**c**) Lifecycle cost for Scenario 2; (**d**) Lifecycle GHG emission for Scenario 2; (**e**) Lifecycle cost for Scenario 3; (**f**) Lifecycle GHG emission for Scenario 3.

3.3.2. Scenario 2—Excess Solar Farm Offset

In Scenario 2 (Figure 7c,d), for the lifecycle cost, the shave factor still has a greater impact than the solar PV size. The optimum shave factor remains at approximately 20% to 25%. However, the optimum solar PV size under this condition increases to approximately 0–100 m^2. For the lifecycle GHG emissions, the solar PV size is critical when the shave

factor is high. The optimum shave factor is approximately 30% to 35%, and the optimum solar PV size is 230 to 245 m^2.

3.3.3. Scenario 3—Excess Solar Grid Selling

In Scenario 3 (Figure 7e,f), for the lifecycle cost, the optimum shave factor remains similar to that in the previous two scenarios, at approximately 20 to 25%. However, the optimum solar PV size under this condition is approximately 150 to 245 m^2. For the lifecycle GHG emissions, the optimum shave factor is lower than that in the previous two scenarios, at approximately 25 to 30%, and the optimum solar PV size is 245 m^2.

3.4. Multi-Objective Optimisation: Pareto Front Solutions

With the lifecycle cost and GHG emission results from the previous section, multi-objective optimisation can be carried out by identifying the Pareto optimum front for the three scenarios and for the three different climatic conditions encountered in the regions with the highest poultry meat production in Australia.

Figure 8 shows the lifecycle cost and lifecycle GHG emissions of Scenario 1 for the reference farm in NSW. In this scenario, it is assumed that there is no storage for the electricity generated by the solar PV panels. The horizontal and vertical axes represent the two objective functions, i.e., the lifecycle cost and the lifecycle GHG emissions, with the data from Figure 8. The different lines formed by the points in the upper right section of Figure 8 show the results obtained when changing the shave factor and fixing the PV size. As shown, the data points are denser on the left than in the upper right section of the plot, because low lifecycle costs and GHG emissions can be achieved by numerous combinations of shave factors and PV sizes. The Pareto optimum solutions are the set of all feasible and efficient choices, but they have trade-offs. The Pareto curve is not expressed in a simple formula but rather defined in this case as the darker line between the two points that correspond to (1) the *minimum* lifecycle *cost* at AUD 220,651, with lifecycle GHG emissions of 490,658 kg CO_2e, achieved with a shave factor of 22% and a PV size of 0 m^2, and (2) the *minimum* lifecycle *GHG emission* at 405,520 kg CO_2e, with a lifecycle cost of AUD 251,686, achieved with a shave factor of 32% and a PV size of 245 m^2.

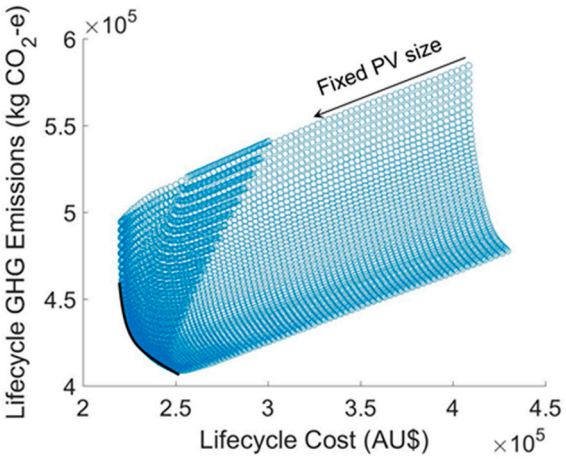

Figure 8. Pareto optimum solutions for Scenario 1 (no electricity storage, no grid sales) in Central Coast, NSW.

Figure 9 shows the lifecycle cost and the lifecycle GHG emissions of Scenario 2 for the reference farm. In this scenario, it is assumed that the electricity generated by the solar PV panels can be offset by the equipment on the farm for up to 10 kW. The trend is similar to that in Scenario 1. In this case, the Pareto optimum solutions are defined as the line between the following two points: (1) the *minimum* lifecycle *cost* at AUD 220,651, with lifecycle GHG emissions of 495,658 kg CO_2e (the same as Scenario 1), achieved with a shave factor of 22% and a PV size of 0 m^2, and (2) the *minimum* lifecycle GHG *emission* at 355,975 kg CO_2e,

with a lifecycle cost of AUD 240,484, achieved with a shave factor of 30% and a PV size of 245 m^2.

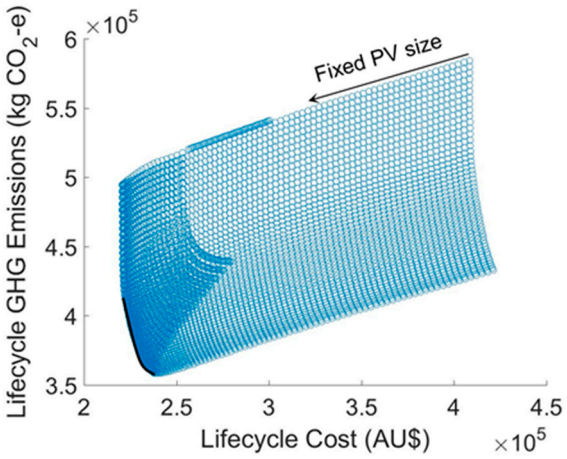

Figure 9. Pareto optimum solutions for Scenario 2 (farm offset) in Central Coast, NSW.

The explanation for there being no solar PV system in both scenarios is that the electricity price on this farm is very competitive, and, thus, adding solar PV panels is not appealing.

Figure 10 shows the lifecycle cost and the lifecycle GHG emissions of Scenario 3 for the reference farm. In this scenario, it is assumed that the electricity generated by the solar PV can be sold back to the grid at market price. The trend is similar to that in both Scenarios 1 and 2. In this case, the Pareto optimum solutions are defined between (1) the minimum lifecycle cost at AUD 208,029, with lifecycle GHG emissions of 201,716 kg CO_2e, achieved with a shave factor of 22% and a PV size of 245 m^2, and (2) the minimum lifecycle GHG emissions at 201,184 kg CO_2e, with a lifecycle cost of approximately AUD 210,421, achieved with a shave factor of 28% and a PV size of 245 m^2. The short line between these two points forms the Pareto optimum front (the difference is minor).

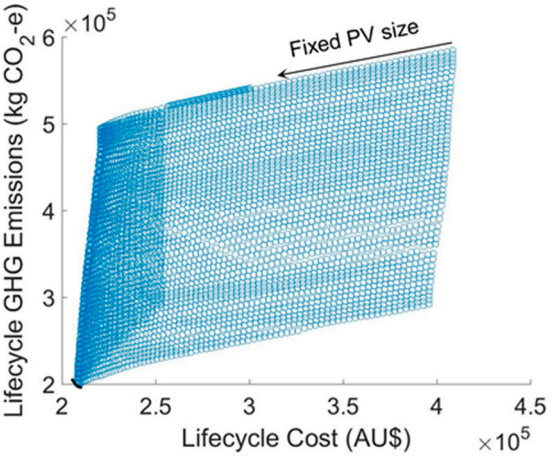

Figure 10. Pareto optimum solutions for Scenario 3 (grid sales) in Central Coast, NSW.

To summarise, the range for the optimum shave factor is similar for all the scenarios tested under NSW weather and pricing structure conditions (approximately 22% to 32%). However, the optimum range for the solar PV panels is different between these scenarios. Scenario 3 has the highest optimum solar PV size (245 m^2), while Scenario 2 has a higher one than Scenario 1. This can be explained as follows: the electricity generated by the solar PV panels can be fully utilised in Scenario 3 (selling to the grid), partially used in Scenario 2

(offset by other equipment on the farm), and barely used in Scenario 1. When the solar PV panels are better used, the capital and maintenance costs of the solar PV panels can be better justified. Hence, the optimum range of the solar PV panels becomes higher.

When observing the Pareto optimum front for the three scenarios on the same scale (Figure 11), it can be clearly seen that Scenario 3 has the best solution, which is because of the full utilisation of the solar PV panels. The optimum lifecycle GHG emissions of Scenario 3 are approximately 40% less than those of Scenario 1 and 60% less than those of the gas-only system. The results reveal that the solar PV panels are essential components, particularly in reducing GHG emissions.

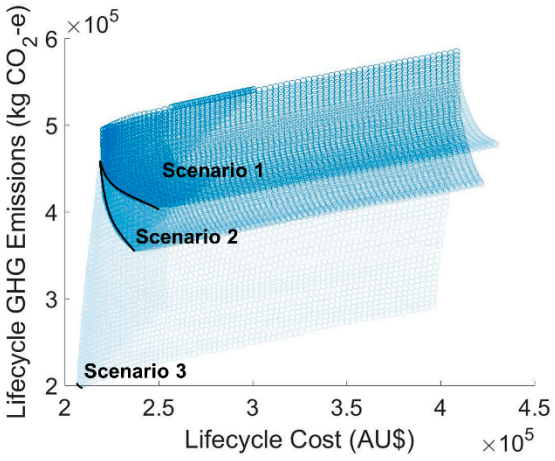

Figure 11. Pareto optimum solutions for three scenarios in Central Coast, NSW.

3.5. Pareto Front Solutions for Other Location and Pricing Scenarios

Using the same methods and approaches mentioned above, this study extends the investigation to state average energy pricing cases for the reference farm in NSW, as well as two other locations (warmer and cooler climates): QLD and VIC. The results (Figure 12 and Table 6) of these cases are discussed below.

Table 6. Optimum lifecycle costs and GHG emissions in different scenarios and locations.

Scenarios		1: No Storage		2: Farm Offset		3: Grid Sales	
		Optimum Cost Case	**Optimum Emissions Case**	**Optimum Cost Case**	**Optimum Emissions Case**	**Optimum Cost Case**	**Optimum Emissions Case**
Central Coast, NSW	Cost, AUD	220,651	251,686	220,651	240,484	208,029	210,421
	GHG Emissions, kg CO_2-e	490,658	405,520	490,658	355,975	201,716	201,184
Central Coast, NSW (SME Pricing)	Cost, AUD	333,003	371,334	311,542	336,202	309,609	322,982
	GHG Emissions, kg CO_2-e	467,775	405,520	404,303	355,975	208,819	201,184
Mornington Peninsula, VIC	Cost, AUD	297,705	355,100	276,575	324,228	257,411	191,595
	GHG Emissions, kg CO_2-e	652,185	505,297	571,395	435,708	244,230	286,375
Sunshine Coast, QLD	Cost, AUD	228,752	259,588	211,119	230,261	212,088	216,462
	GHG Emissions, kg CO_2-e	242,179	233,320	192,615	169,725	4179	−15,847

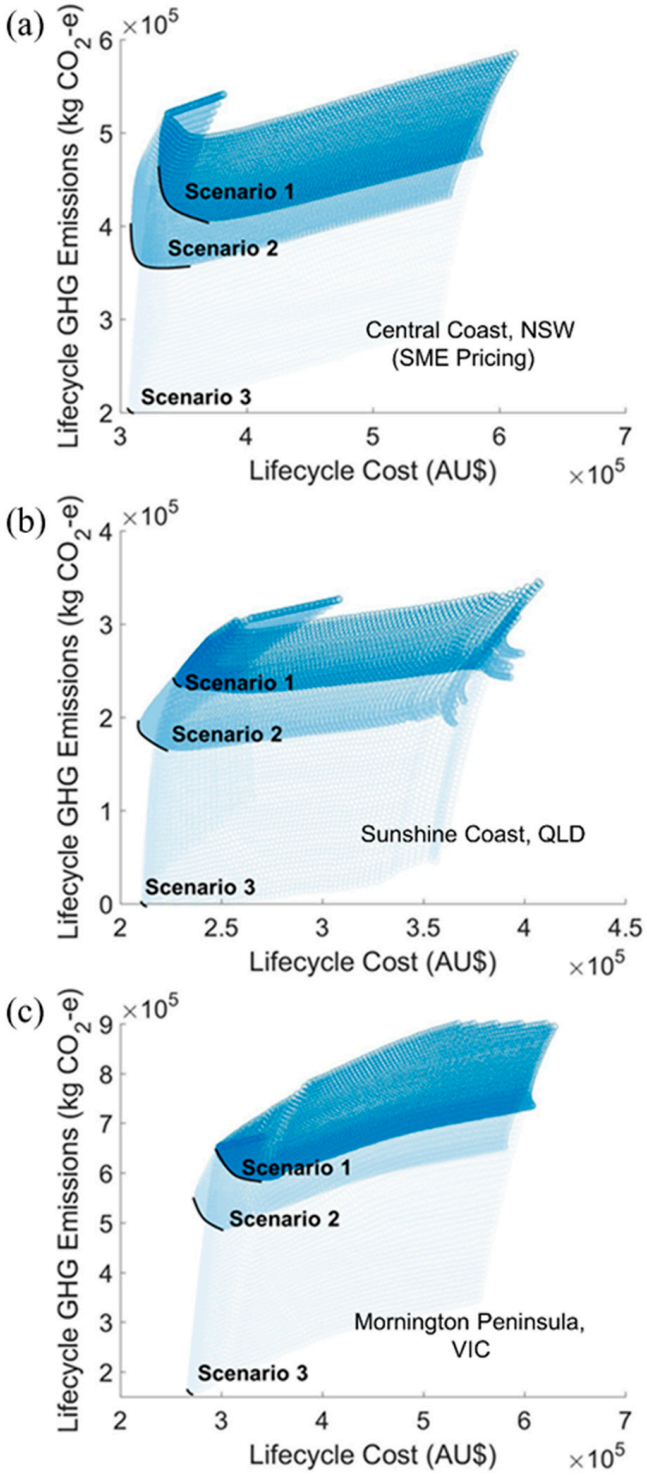

Figure 12. Pareto optimum solutions for average pricing cases in (**a**) Central Coast, NSW; (**b**) Sunshine Coast, QLD; and (**c**) Mornington Peninsula, VIC. Please note the different axis scales for each case.

Among all three scenarios, Scenario 3 shows the best Pareto optimum solution, which is due to the full utilisation of the solar PV panels. Considering the optimum lifecycle cost, all the scenarios in the three cases show about 45% to 55% savings for the gas-only system. For the optimum lifecycle GHG emissions, Scenario 3 in all three cases shows a significant advantage. Regarding the NSW case, the optimum lifecycle GHG emissions in Scenario 3 are approximately 60% lower than those in Scenario 1 and 40% lower than those in Scenario 2. Regarding the VIC case, the optimum lifecycle GHG emissions in

Scenario 3 are approximately 75% lower than those in Scenario 1 and 60% lower than those in Scenario 2. Regarding the QLD case, the optimum lifecycle GHG emissions in Scenario 3 can be reduced to 0, which is partly because of the relatively low heat demand of QLD. These results confirm that solar PV panels are essential in reducing GHG emissions.

When considering the shave factor and solar PV size under the optimum conditions, similar patterns to the case discussed in Section 3.5 are observed. The optimum shave factors range from approximately 20% (VIC) to 35% (QLD) for these cases. For the optimum solar PV size, almost all cases require the largest size in Scenario 3 (245 m^2), a smaller size in Scenario 2 (100 to 245 m^2), and the smallest size in Scenario 1 (0 to 125 m^2). These findings are also in good agreement with the findings in Section 3.5.

3.6. Applicability of Results to Other Worldwide Locations in Similar Climate Zones

As mentioned earlier, the locations of the three case studies investigated fall into humid subtropical (Sunshine Coast, QLD, Australia, and Central Coast, NSW, Australia) and temperate oceanic (Mornington Peninsula, VIC, Australia) climate zones of the Köppen classification [21]. This work aimed to highlight the technical solution's applicability to other parts of the world. As this classification is based on threshold values and the seasonality of monthly ambient air temperature and precipitation, which are essential for the performance of GSHP and solar PV systems, the hybrid system performance can be reasonably similar in one climate zone [55,56]. Therefore, it is expected that the technical solution would have a similar effect in other parts of the world. These two climate zones include Western Europe and south-eastern parts of the United States, China, Africa, and Australia, as well as isolated locations elsewhere. The key findings of this research can potentially be applied to the poultry industry in these regions.

3.7. Future Considerations for Improvements in Energy Efficiency

With the continuous development of energy technology, significant improvements in the energy efficiency of various energy systems are expected. With the hybrid geothermal–solar–gas system under investigation in this study, it is reasonable to expect enhancements in the COP of GSHPs. While it may be challenging to provide a comprehensive quantitative analysis regarding this trend, a qualitative discussion for future considerations can be provided.

Concerning the improvement of COP for GSHPs, the data on heat pump performance applied in this study are obtained from the specifications of the heat pumps employed in the NSW case study. As depicted in Figure 6, the COP exhibits a decreasing trend with an increasing shave factor based on TRNSYS simulations considering various scenarios. As technology progresses and COP values improve, a corresponding upward shift in the COP trend can be expected. However, since the ground loop infrastructure is typically installed once and remains fixed, the potential replacement of existing heat pumps with more efficient models in the future may only result in marginal reductions in the operational costs and greenhouse gas (GHG) emissions of the system. This aspect constitutes a relatively small fraction of the overall lifecycle cost and GHG emissions, as illustrated in Figures 12 and 13. Consequently, the impact of improved COP values on the Pareto optimum will probably range from minimal to negligible, depending on the specific circumstances and the extent to which the electricity generated by solar PV panels offsets energy demands.

As an example, Figure 13 presents a hypothetical analysis, which is conducted based on Scenario 1 concerning the case in Mornington Peninsula, VIC, as delineated in Figure 12c (illustrated in Figure 13a,c,e). An additional theoretical scenario is examined wherein the coefficient of performance (COP) of the ground-source heat pumps (GSHPs) demonstrates an increase of 0.5 across the entire lifecycle (depicted in Figure 13b,d,f).

Observations from Figure 13a–d reveal that the Pareto optimal solutions—represented by the blue regions in the diagrams—remain consistent, albeit with a slight reduction in both cost and emissions (as shown in Figure 13e,f). This analysis conclusively indicates that, despite enhancements in energy technology, particularly in the domain of GSHPs,

resulting in marginal modifications to Pareto optimum frontiers, the fundamental trends and principles guiding system optimisation and Pareto optimum solutions are expected to remain largely intact.

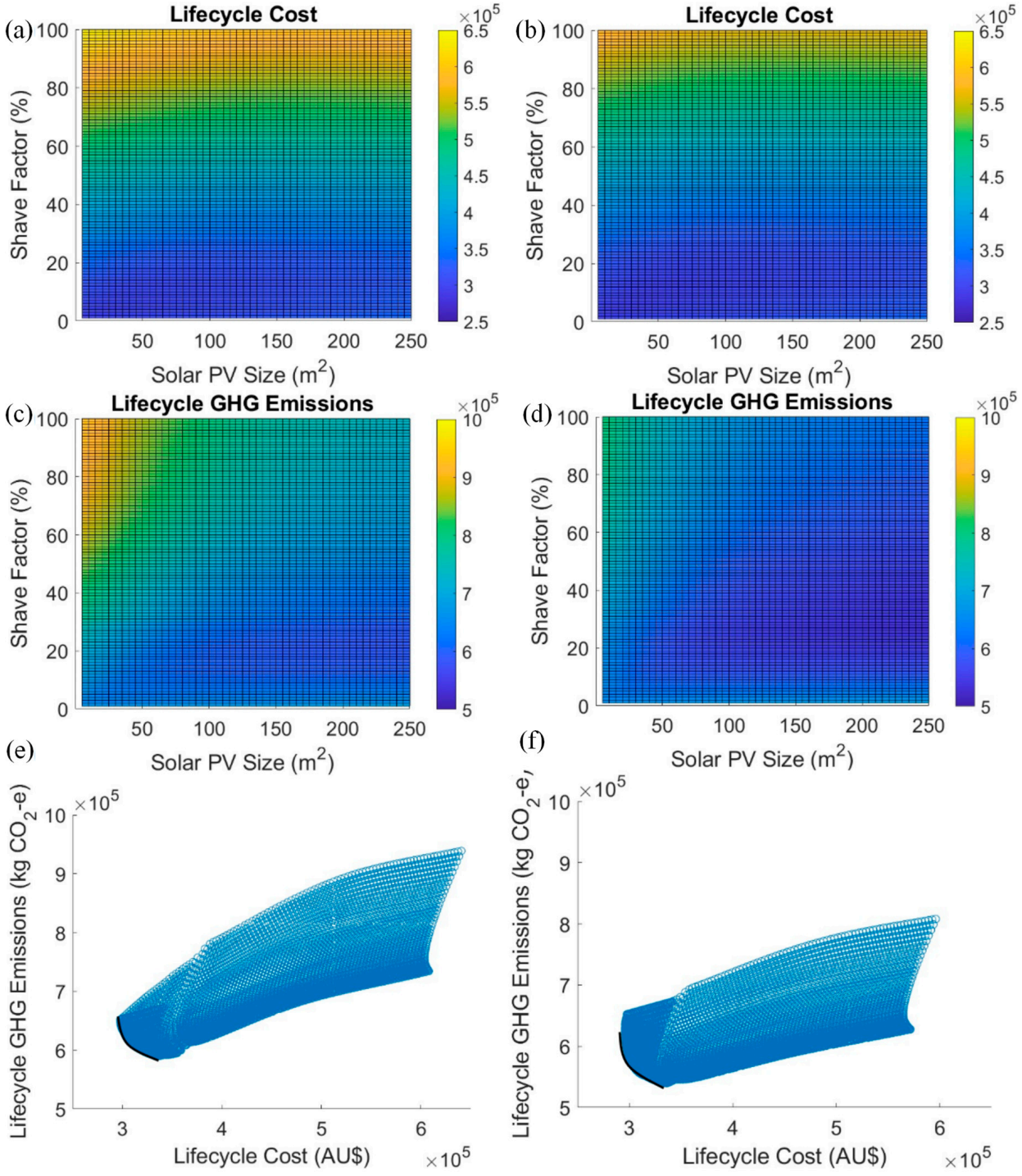

Figure 13. Hypothetical comparison based on Scenario 1 of case in Mornington Peninsula, VIC: (**a**) lifecycle cost of original case, (**b**) lifecycle cost of increased energy efficiency case, (**c**) lifecycle GHG emissions of original case, (**d**) lifecycle GHG emissions of increased energy efficiency case, (**e**) Pareto optimum for original case, and (**f**) Pareto optimum for increased energy efficiency case.

4. Conclusions

This work conducted a comprehensive evaluation of the unique annual heating load pattern of poultry sheds in humid subtropical and temperate oceanic climate zones in Australia. The investigation was exemplified by case studies covering 74.4% of national chicken meat production, specifically in the Central Coast (NSW), Sunshine Coast (QLD), and Mornington Peninsula (VIC). A hybrid geothermal–solar (PV)–gas system was proposed as an energy-efficient and cost-effective heating solution for the sheds. Based on verified hourly heating loads simulated using TRNSYS, the hybrid heating system was analysed in terms of various shave factors and solar PV panel sizes.

To quantify the annual performance of the system, hourly coefficients of performance (COPs) of the ground-source heat pumps (GSHPs) were simulated using the developed TRNSYS model. The annual electricity generated by the solar PV panels was calculated based on the optimum slopes of the panels. In these systems, the baseload heating demand was satisfied by the GSHPs, with the solar photovoltaic panels providing the electricity needed to drive the pumps and the liquefied petroleum gas (LPG) gas boilers topping up the balance of the heating.

Lifecycle cost and greenhouse gas (GHG) emission analyses were performed to optimise the sizes of the components of the hybrid geothermal system and determine the most cost-effective configuration with the lowest GHG emissions. Multi-objective optimisations (minimum lifecycle cost and minimum GHG emissions) were conducted to identify the Pareto front solutions for three different scenarios. As the feasible search region was relatively small, a full enumeration method was used.

The results indicate that considerable reductions in lifecycle heating costs (up to 55%) and GHG emissions (up to 50%) could be achieved when optimised hybrid systems are used for poultry shed heating. The Pareto front solutions for this hybrid geothermal–solar–gas heating system were also determined. By comparing the Pareto front solutions in different scenarios, it was found that the shave factor, a measure of the proportion of GSHP to the overall heating system, had the highest impact on reducing the lifecycle cost, while the size and utilisation of the solar PV panels contributed more to reducing the lifecycle GHG emissions. This work provides valuable insights for the design and optimisation of energy-efficient and cost-effective heating systems for rural industry in different climate zones.

Author Contributions: Conceptualization, Y.Z., G.A.N. and L.A.; methodology, Y.Z., G.A.N. and L.A.; software, Y.Z., G.A.N. and L.A.; validation, Y.Z., G.A.N. and L.A.; formal analysis, Y.Z., G.A.N., K.S. and L.A.; investigation, Y.Z., G.A.N., K.S. and L.A.; resources, G.A.N., K.S. and L.A.; writing—original draft preparation, Y.Z., G.A.N., K.S. and L.A.; writing—review and editing, Y.Z., G.A.N., K.S. and L.A; visualization, Y.Z. and G.A.N.; supervision, G.A.N. and L.A.; project administration, G.A.N. and L.A.; funding acquisition, G.A.N., K.S. and L.A. All authors have read and agreed to the published version of the manuscript.

Funding: The authors would like to thank the Australian Research Council for the funding of Linkage Project LP160100070 and FT140100227, and industry partners Ground Source Systems Pty Ltd. and Golder Associates Pty Ltd.

Data Availability Statement: The original contributions presented in the study are included in the article, further inquiries can be directed to the corresponding author/s.

Conflicts of Interest: The authors declare no conflicts of interest.

Appendix A. Hourly Solar PV Panel Electricity Generation Calculation Method

The equations below are used to calculate the electricity generated hourly by the solar PV panels. The primary aim of the calculation is to determine the irradiation on the sloped surface of the solar PV panel I_T, which is calculated as follows [57]:

$$I_T = RI = \left[\frac{I_b}{I}R_b + \frac{I_d}{I}\left(\frac{1+cos\beta}{2}\right) + \rho_g\left(\frac{1-cos\beta}{2}\right)\right]\cdot I \quad \text{(A1)}$$

Here, R is the ratio of the total radiation on the sloped surface to that on a horizontal surface; I is the total hourly irradiation on a horizontal surface in MJ·m^{-2}·h^{-1}, which equals $I_b + I_d$; I_b is the hourly beam irradiation on a horizontal surface in MJ·m^{-2}·h^{-1}; I_d is the hourly diffuse irradiation on a horizontal surface in MJ·m^{-2}·h^{-1}; β is the slope in degrees; ρ_g is the dimensionless reflectance of the ground (ground albedo) [58]; and R_b is the ratio of the beam radiation on a slope surface to that on the horizontal plane, and it can be calculated as follows [57]:

$$R_b = \frac{\cos(\varnothing + \beta)cos\delta cos\omega + \sin(\varnothing + \beta)sin\delta}{cos\varnothing cos\delta cos\omega + sin\varnothing sin\delta} \text{ (for North facing surfaces)} \quad \text{(A2)}$$

Here, ∅ is the latitude in degrees; β is the slope in degrees as mentioned above; δ is the declination angle in degrees, which represents the angular position of the sun at noon with respect to the plane of the equator; and ω is the hour angle in degrees, which represents the angular displacement of the sun east or west of the local meridian due to the rotation of the Earth on its axis.

The equations show that the energy generation of the solar PV panels is related to the slope of the solar PV panels. Further analysis is needed to determine the optimum slope. The weather data used in this analysis are the same as the "Meteonorm" data explained in the previous sections. The optimum slope for the solar PV panel is determined. By varying the slope from 0° to 90° degrees in 0.1° steps, a total annual electricity generation of 5 m^2 (1.2 kW capacity) is calculated, using the parameters of the solar PV panels summarised in Table A1. For example, the optimum slope for the site in Central Coast, NSW, is determined to be 39°. The optimum slopes for Mornington Peninsula, VIC, and Sunshine Coast, QLD, are 34° and 26°, respectively. Then, Equation (A3) can be used to calculate the instantaneous array efficiency of the solar PV panels [57]:

$$\eta = \eta_r[1 - \beta_t(t_c - t_r)]\eta_{pt} \quad \text{(A3)}$$

Here, η_r is the cell packing factor times the cell reference efficiency; β_t is the temperature coefficient of efficiency; t_c is the cell temperature; t_r is the reference temperature; and η_{pt} is the efficiency of the power tracking equipment.

Table A1. Parameters of solar PV panel used in this investigation.

NOCT	45	Nominal operating cell temperature, °C
η_r	0.122	Cell packing factor x cell packing efficiency
η_{pt}	1	Efficiency of power tracking equipment
β_t	0.0065	Temperature coefficient of efficiency
t_r	25	Reference temperature, °C

Figure A1 shows the hourly solar radiation on the surface (from the TMY data) and the hourly electricity generation of the PV panels discussed above (see Table 6). It can be seen in the figure that the solar radiation is higher in the summer (with a peak radiation of 7.5 MJ·m^{-2}·h^{-1} in February) than in the winter (the highest radiation in July is only approximately 5.5 MJ·m^{-2}·h^{-1}). However, the amount of electricity generated in the different seasons differs only marginally. As the solar PV panels typically have an optimum temperature at about 25 °C (when above and below this temperature, the efficiency of the solar PV panel decreases), this marginal difference between summer and winter solar PV power generation could possibly be because, in summer, the higher outdoor air temperature reduces the efficiency of the solar PV panels [57].

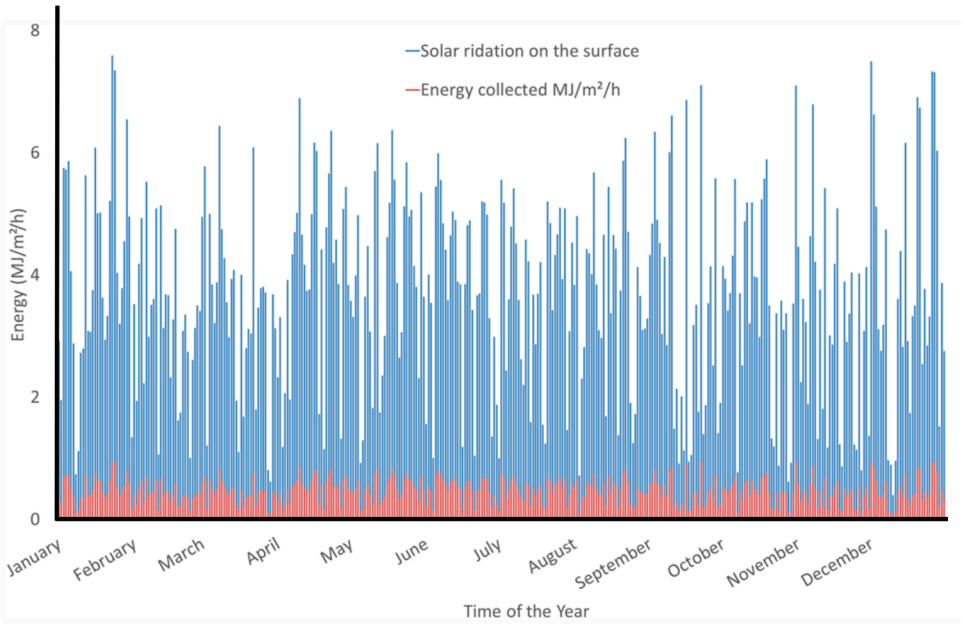

Figure A1. Hourly radiation and electricity generation of solar PV panels in Central Coast, NSW.

References

1. Johnston, I.W.; Narsilio, G.A.; Colls, S. Emerging geothermal energy technologies. *KSCE J. Civ. Eng.* **2011**, *15*, 643–653. [CrossRef]
2. Han, C.; Yu, X.B. Performance of a residential ground source heat pump system in sedimentary rock formation. *Appl. Energy* **2016**, *164*, 89–98. [CrossRef]
3. Zhou, Z.; Zhang, Z.; Chen, G.; Zuo, J.; Xu, P.; Meng, C.; Yu, Z. Feasibility of ground coupled heat pumps in office buildings: A China study. *Appl. Energy* **2016**, *162*, 266–277. [CrossRef]
4. Lund, J.W.; Toth, A.N. Direct utilization of geothermal energy 2020 worldwide review—ScienceDirect. *Geothermics* **2020**, *90*, 101915. [CrossRef]
5. Kharseh, M.; Nordell, B. Sustainable heating and cooling systems for agriculture. *Int. J. Energy Res.* **2011**, *35*, 415–422. [CrossRef]
6. Choi, H.C.; Salim, H.M.; Akter, N.; Na, J.C.; Kang, H.K.; Kim, M.J.; Kim, D.W.; Bang, H.T.; Chae, H.S.; Suh, O.S. Effect of heating system using a geothermal heat pump on the production performance and housing environment of broiler chickens. *Poult. Sci.* **2012**, *91*, 275–281. [CrossRef] [PubMed]
7. Eslami-Nejad, P.; Bernier, M. Coupling of geothermal heat pumps with thermal solar collectors using double U-tube boreholes with two independent circuits. *Appl. Therm. Eng.* **2011**, *31*, 3066–3077. [CrossRef]
8. Kjellsson, E.; Hellström, G.; Perers, B. Optimization of systems with the combination of ground-source heat pump and solar collectors in dwellings. *Energy* **2010**, *35*, 2667–2673. [CrossRef]
9. Weeratunge, H.; Narsilio, G.; De Hoog, J.; Dunstall, S.; Halgamuge, S. Model predictive control for a solar assisted ground source heat pump system. *Energy* **2018**, *152*, 974–984. [CrossRef]
10. Lu, Q.; Narsilio, G.A.; Aditya, G.R.; Johnston, I.W. Economic analysis of vertical ground source heat pump systems in Melbourne. *Energy* **2017**, *125*, 107–117. [CrossRef]
11. Alavy, M.; Nguyen, H.V.; Leong, W.H.; Dworkin, S.B. A methodology and computerized approach for optimizing hybrid ground source heat pump system design. *Renew. Energy* **2013**, *57*, 404–412. [CrossRef]
12. Gang, W.; Wang, J.; Wang, S. Performance analysis of hybrid ground source heat pump systems based on ANN predictive control. *Appl. Energy* **2014**, *136*, 1138–1144. [CrossRef]
13. Kuzmic, N.; Law, Y.L.E.; Dworkin, S.B. Numerical heat transfer comparison study of hybrid and non-hybrid ground source heat pump systems. *Appl. Energy* **2016**, *165*, 919–929. [CrossRef]
14. Man, Y.; Yang, H.; Wang, J. Study on hybrid ground-coupled heat pump system for air-conditioning in hot-weather areas like Hong Kong. *Appl. Energy* **2010**, *87*, 2826–2833. [CrossRef]
15. Mikhaylova, O.; Choudhary, R.; Soga, K.; Johnston, I.W. Benefits and Optimisation of District Hybrid Ground Source Heat Pump Systems. In *Energy Geotechnics*; Taylor & Francis: Abingdon, UK, 2016; pp. 535–541.
16. Woo, N.S.; Kim, Y.J.; Jo, Y.D.; Hwang, I.J. Performance investigation of the hybrid-renewable energy system with geothermal and solar heat sources for a residential building in South Korea. *J. Sol. Energy Eng.* **2013**, *135*, 021005. [CrossRef]
17. Yi, M.; Hongxing, Y.; Zhaohong, F. Study on hybrid ground-coupled heat pump systems. *Energy Build.* **2008**, *40*, 2028–2036. [CrossRef]
18. Central Intelligence Agency. *The World Factbook 2019*; Central Intelligence Agency: Washington, DC, USA, 2019.
19. National Farmer's Federation. *NFF Annual Review 2014–15*; National Farmer's Federation: Canberra, Australia, 2016.

20. National Farmer's Federation. *Farm Facts*; National Farmer's Federation: Canberra, Australia, 2012.
21. Australian Bureau of Statistics. *7215.0—Livestock Products, Australia, March 2016*; Australian Bureau of Statistics: Canberra, Australia, 2016.
22. Zhou, Y.; Bidarmaghz, A.; Narsilio, G.; Aye, L. Heating and Cooling Loads of a Poultry House in Central Coast, NSW, Australia. In Proceedings of the World Sustainable Built Environment Conference 2017, Hong Kong, 5–7 June 2017.
23. Ball, A.; Ahmad, S.; McCluskey, C.; Pham, P.; Ahn, I.; Dawson, L.; Nguyen, T.; Nowakowski, D. *Australian Energy Update 2016*; Department of the Environment and Energy: Canberra, Australia, 2016.
24. Regulator, A.E. *National Greenhouse Accounts Factors, in Australian National Greenhouse Accounts*; Australian Government, Department of the Enviroment: Canberra, Australia, 2017.
25. Bakirci, K.; Ozyurt, O.; Comakli, K.; Comakli, O. Energy analysis of a solar-ground source heat pump system with vertical closed-loop for heating applications. *Energy* **2011**, *36*, 3224–3232. [CrossRef]
26. Esen, H.; Esen, M.; Ozsolak, O. Modelling and experimental performance analysis of solar-assisted ground source heat pump system. *J. Exp. Theor. Artif. Intell.* **2017**, *29*, 1–17. [CrossRef]
27. Si, Q.; Okumiya, M.; Zhang, X. Performance evaluation and optimization of a novel solar-ground source heat pump system. *Energy Build.* **2014**, *70*, 237–245. [CrossRef]
28. Trillat-Berdal, V.; Souyri, B.; Achard, G. Coupling of geothermal heat pumps with thermal solar collectors. *Appl. Therm. Eng.* **2007**, *27*, 1750–1755. [CrossRef]
29. Zhou, Y.; Mikhaylova, O.; Bidarmaghz, A.; Donovan, B.; Guillermo, N.; Aye, L. Hybrid geothermal-gas and geothermal-solar-gas heating systems for poultry sheds. In Proceedings of the Zero Energy Mass Custom Home 2018, Melbourne, Australia, 29 January–1 February 2018.
30. Sarbu, I.; Sebarchievici, C. General review of ground-source heat pump systems for heating and cooling of buildings. *Energy Build.* **2014**, *70*, 441–454. [CrossRef]
31. Hong, B.; Howarth, R.W. Greenhouse gas emissions from domestic hot water: Heat pumps compared to most commonly used systems. *Energy Sci. Eng.* **2016**, *4*, 123–133. [CrossRef]
32. Australian Chicken Meat Federation (ACMF) Inc. *An Industry in Profile*; Australian Chicken Meat Federation (ACMF) Inc.: North Sydney, Australia, 2016.
33. Kottek, M.; Grieser, J.; Beck, C.; Rudolf, B.; Rubel, F. World map of the Köppen-Geiger climate classification updated. *Meteorol. Z.* **2006**, *15*, 259–263. [CrossRef] [PubMed]
34. Singh, H. Optimizing delivery of genetic merit in subtropical climates through advanced reproductive technologies. *Poult. Sci.* **1999**, *78*, 453–458. [CrossRef] [PubMed]
35. Rowlinson, P. Adapting livestock production systems to climate change–temperate zones. In Proceedings of the Livestock and Global Climate Change, Hammamet, Tunisia, 17–20 May 2008; pp. 61–63.
36. Meteotest. *Meteonorm Handbook*; Meteotest: Bern, Switzerland, 2016.
37. Department of Meteorology. *Australian Climate Data*; Department of Meteorology: Canberra, Australia, 2018.
38. Zhou, Y.; Narsilio, G.; Makasis, N.; Soga, K.; Chen, P.; Aye, L. Artificial neural networks for predicting the performance of heat pumps with horizontal ground heat exchangers. *Front. Energy Res.* **2024**, *12*, 1423695.
39. Zhou, Y.; Bidarmaghz, A.; Makasis, N.; Narsilio, G. Ground-source heat pump systems: The effects of variable trench separations and pipe configurations in horizontal ground heat exchangers. *Energies* **2021**, *14*, 3919. [CrossRef]
40. Vest, L.; Tyson, B. *Key Factors for Poultry House Ventilation*; Bulletin-Cooperative Extension Service, University of Georgia, College of Agriculture (USA): Athens, GA, USA, 1991.
41. Alviss Consulting and Energy Consumers Australia. *Analysis of Small Business Retail Energy Bills in Australia*; Alviss Consulting and Energy Consumers Australia: Melbourne, Australia, 2017.
42. JACOBS and Australian Energy Market Operator. *Retail Electricity Price History and Projected Trends*; Australian Energy Market Operator: Melbourne, Australia, 2017.
43. Krauter, S.; Rüther, R. Considerations for the calculation of greenhouse gas reduction by photovoltaic solar energy. *Renew. Energy* **2004**, *29*, 345–355. [CrossRef]
44. Leckner, M.; Zmeureanu, R. Life cycle cost and energy analysis of a Net Zero Energy House with solar combisystem. *Appl. Energy* **2011**, *88*, 232–241. [CrossRef]
45. Nawaz, I.; Tiwari, G. Embodied energy analysis of photovoltaic (PV) system based on macro-and micro-level. *Energy Policy* **2006**, *34*, 3144–3152. [CrossRef]
46. Magraner, T.; Montero, A.; Quilis, S.; Urchueguía, J.F. Comparison between design and actual energy performance of a HVAC-ground coupled heat pump system in cooling and heating operation. *Energy Build.* **2010**, *42*, 1394–1401. [CrossRef]
47. Lu, Q. *Shallow Geothermal System: Feasibility and Design Practices in Melbourne, Australia*; University of Melbourne: Melbourne, Australia, 2018.
48. Kirk, S.J.; Dell'Isola, A.J. *Life Cycle Costing for Design Professionals*; McGraw-Hill: New York, NY, USA, 1995.
49. Markvart, T. *Solar Electricity*; University of Southampton: Southampton, UK; John Wiley and Sons Ltd.: Chichester, UK, 1994.
50. Greenwell, T. The economic challenge. *J. Aust. Polit. Econ.* **2024**, *92*, 9–34.

51. Colangelo, G.; Congedo, P.; Starace, G. Horizontal heat exchangers for GSHP. Efficiency and cost investigation for three different applications. In Proceedings of the ECOS 2005: The 18th International Conference on Efficiency, Cost, Optimization, Simulation and Environmental Impact of Energy Systems, Trondheim, Norway, 20–22 June 2005.
52. Omer, A.M. Ground-source heat pumps systems and applications. *Renew. Sustain. Energy Rev.* **2008**, *12*, 344–371. [CrossRef]
53. In, S.; Cho, K.; Lim, B.; Lee, C. Partial load performance test of residential heat pump system with low-GWP refrigerants. *Appl. Therm. Eng.* **2015**, *85*, 179–187. [CrossRef]
54. Waddicor, D.A.; Fuentes, E.; Azar, M.; Salom, J. Partial load efficiency degradation of a water-to-water heat pump under fixed set-point control. *Appl. Therm. Eng.* **2016**, *106*, 275–285. [CrossRef]
55. Belda, M.; Holtanová, E.; Halenka, T.; Kalvová, J. Climate classification revisited: From Köppen to Trewartha. *Clim. Res.* **2014**, *59*, 1–13. [CrossRef]
56. Panagiotidou, M.; Aye, L.; Rismanchi, B. Solar driven water heating systems for medium-rise residential buildings in urban mediterranean areas. *Renew. Energy* **2020**, *147*, 556–569. [CrossRef]
57. Duffie, J.A.; Beckman, W.A. *Solar Engineering of Thermal Processes*; John Wiley & Sons: Hoboken, NJ, USA, 2013.
58. Gueymard, C.A. Direct and indirect uncertainties in the prediction of tilted irradiance for solar engineering applications. *Sol. Energy* **2009**, *83*, 432–444. [CrossRef]